Chapter 9

Purification and Application of a Small Actin Probe for Single-Molecule Localization Microscopy

Roderick P. Tas, Trusanne G.A.A. Bos, and Lukas C. Kapitein

Abstract

The cytoskeleton is involved in many cellular processes. Over the last decade, super-resolution microscopy has become widely available to image cytoskeletal structures, such as microtubules and actin, with great detail. For example, Single-Molecule Localization Microscopy (SMLM) achieves resolutions of 5–50 nm through repetitive sparse labeling of samples, followed by Point-Spread-Function analysis of individual fluorophores. Whereas initially this approach depended on the controlled photoswitching of fluorophores targeted to the structure of interest, alternative techniques now depend on the transient binding of fluorescently labeled probes, such as the small polypeptide lifeAct that can transiently interact with polymerized actin. These techniques allow for simple multicolor imaging and are no longer limited by a fluorophore's blinking properties. Here we describe a detailed step-by-step protocol to purify, label, and utilize the lifeAct fragment for SMLM. This purification and labeling strategy can potentially be extended to a variety of protein fragments compatible with SMLM.

Key words Actin, Sample fixation, Fluorophores, Super-resolution microscopy, Exchangeable probe

1 Introduction

Cellular morphology, migration, division, polarization, and differentiation are all processes that require very specific cytoskeleton organization and dynamics. The exact organization of microtubules and actin directly influences the available roads for active transport by kinesins/dyneins and myosins, respectively [1–3]. A specific actin organization is important during cell migration, neuronal growth cone extension, brush border formation, and many other processes [4, 5]. Different actin structures underlie different functions. For example, while dense structures of actin in the axon initial segment of neurons can mediate myosin-mediated anchoring of cargoes, cortical actin structures can drive directional motility in epithelial cells [6, 7]. Therefore, understanding the nanoscale organization of the actin and microtubule

Erwin J.G. Peterman (ed.), *Single Molecule Analysis: Methods and Protocols*, Methods in Molecular Biology, vol. 1665, DOI 10.1007/978-1-4939-7271-5_9,

cytoskeleton is important to understand the mechanisms and functions of these specialized structures.

Conventional fluorescence microscopy is widely available and continues to be a powerful tool to provide new insights in cytoskeleton organization and dynamics. Better objectives, faster cameras as well as genetic tools, and immunocytochemistry can be used to label and image individual proteins with high specificity and temporal resolution. However, conventional fluorescent microscopy is limited by the diffraction of light, which causes fluorophores to be imaged as a spatially extended structure of 200–300 nm. This detected pattern of a single fluorophore on the camera is called the Point Spread Function (PSF) which is shaped like an airy disk. When two fluorophores emit light at the same time while they are very close, the airy disks overlap and cannot be separated. This phenomenon limits the distance at which you can separate two fluorophores or structures to approximately half the wavelength of the detected light.

During the last decade several fluorescence-based microscopy techniques have been developed that are not limited by diffraction [8, 9]. Single-molecule localization microscopy (SMLM) is a super-resolution technique based on the sequential detection of individual fluorophores and subsequent midpoint determination with nanometer precision. All detected fluorophores that label the structure of interest can result in a single reconstructed image where all fluorophore locations are plotted with high precision [10]. Techniques that are based on SMLM are PALM (Photoactivated Localization Microscopy—[11]), STORM (Stochastic Optical Reconstruction Microscopy—[10]), dSTORM (direct STORM—[12]), GSDIM (Ground-State-Depletion and Single-Molecule return—[13]), and PAINT (Point Accumulation for Imaging in Nanoscale Topography—[14]). In fixed samples (d)STORM provides the highest resolution and is therefore commonly used to study the exact architecture of the cytoskeleton beyond the diffraction limit. One important breakthrough was the discovery of the periodic actin and spectrin rings in the axon [15]. A major limitation of dSTORM is the limited number of fluorophores compatible with robust multicolor imaging. Another limitation of dSTORM is the use of high laser intensities to bring the majority of the fluorophores in a dark-state so that individual molecules can be detected. This results in overall bleaching of fluorophores and reduces the amount of detections over time. Additionally, achieving such high laser intensities often requires illumination of only a small area of the sample.

PAINT-like methods overcome these limitations. They rely on the transient binding of fluorophores targeted to the structure of interest. Weakly interacting probes coupled to a fluorophore will bind stochastically, serve as point emitter for a limited time and diffuse back into solution (Fig. 1a) [16]. The imaging solution can

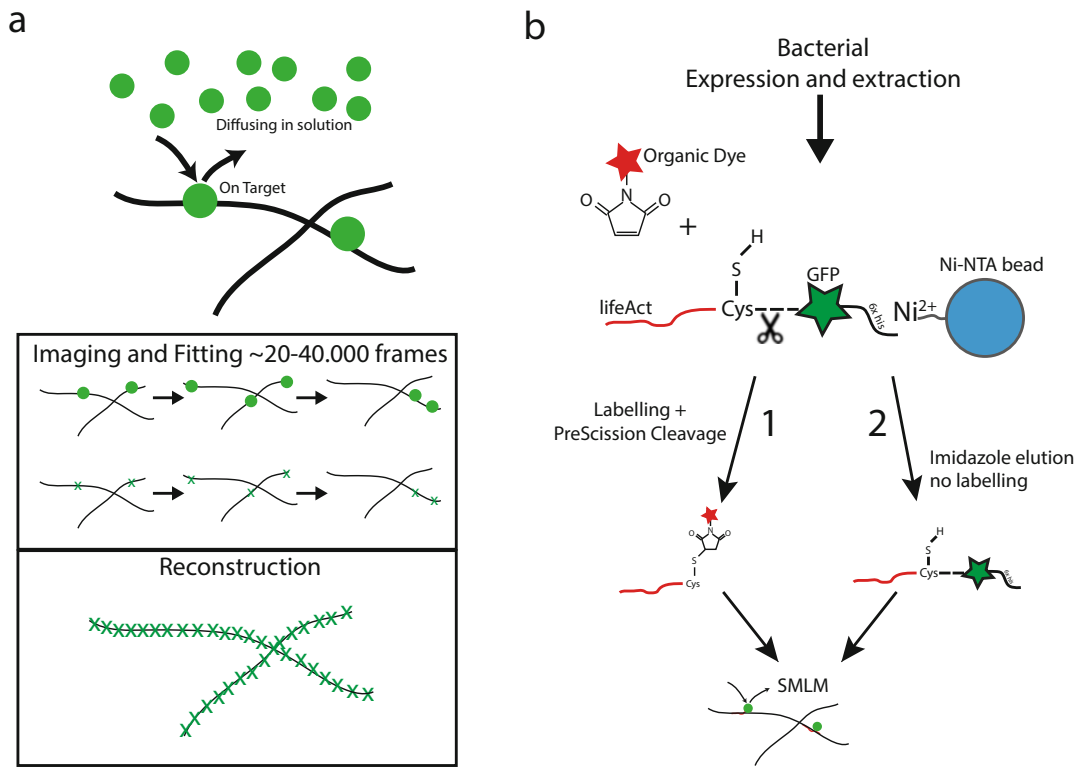

Fig. 1 Single-molecule localization microscopy (SMLM) by transient binding. (**a**) Principle of SMLM by transient binding. From solution, fluorophores targeted by a specific molecule transiently bind to the structure of interest so that single molecules can be observed. These single-molecule events are recorded through time. Subsequently midpoint determination and reconstruction lead to a super-resolved image. (**b**) Schematic representation of the purification and labeling lifeAct probe with GFP or organic dyes to label actin. *Arrow 1* represents purification through proteolytic cleavage. *Arrow 2* represents the purification with a GFP as fluorescent protein. Dashed line with scissors indicates PreScission cleavage site

then be washed and a second structure can be imaged using a similar or different fluorophore targeted to a different structure. The overall advantage of this technique lies within the transient binding. Unlike dSTORM, there is no need for high laser intensities to bring the majority of fluorophores to a dark state. In addition, the probes on the target are continuously replaced by fresh probes from solution resulting in a continuing imaging cycle not limited by bleaching. Furthermore, PAINT-like SMLM can be performed using a wide variety of fluorophores for multicolor imaging.

A limiting factor for PAINT-type approaches is the need for proper transiently interacting probes. Recently, a generic approach for PAINT, DNA-PAINT, was introduced in which structures labeled with an antibody conjugated to single-stranded DNA can be imaged very specifically with complementary DNA coupled to a

fluorophore [14]. Alternatively, protein–protein interactions can be used to target fluorophores to the desired structure. It has been shown that using small protein fragments/peptides coupled to a fluorophore, SMLM by transient binding could be performed on actin and other cytoskeleton structures. The major advantage of these interactions is that they are highly specific and can rely on very small probes. Recent work showed that using these transient protein–protein interactions, the actin cytoskeleton can be visualized in high detail by lifeAct coupled to an Atto-dye [17]. LifeAct is a small 17-amino acid fragment of the yeast Abp140 protein that was found to label actin [18]. Whereas this work used a commercially obtained synthesized lifeAct probe, we recently developed an approach to purify the lifeAct peptide, either fused to fluorescent proteins or conjugated with organic dyes after purification.

Here we describe a step-by-step protocol to purify the lifeAct domain for super-resolution microscopy. This method allows for SMLM using either a fused fluorescent protein or using any organic fluorophore coupled by thiol–maleimide chemistry. For this a construct that consists of "lifeAct-Cysteine-PreScission Cleavage Site-GFP-6× His" was created, as shown in Fig. 1. To perform SMLM using the fluorescent protein module (GFP) a rapid his-tag purification can be performed. To functionalize the small peptide with any organic dye, thiol–maleimide chemistry on the introduced cysteine and subsequent proteolytic cleavage by PreScission protease can be performed (Fig. 1b). The generation of this versatile probe can be extended to other protein fragments to label other structures of interest.

2 Materials

All imaging experiments are performed at room temperature unless indicated otherwise. Solutions are dissolved in ultrapure water (~18 MΩ cm at 25 °C). During purification, buffers and samples are kept on ice to avoid protein degradation.

2.1 Purification and Labeling

1. *E. coli* BL21DE3 transformed with an IPTG inducible expression vector for lifeAct-cys-PreScission Site-GFP-6×His (*see* **Note 1**).
2. Resuspension/lysis Buffer: 20 mM HNa_2PO_4, 300 mM NaCl, 0.5% glycerol, 7% glucose, EDTA-free protease inhibitor (Roche Diagnostics GmbH), 1 mM dithiothreitol (DTT), pH 7.4. To a beaker containing a magnetic stir bar, add 100 ml water, 0.71 g of HNa_2PO_4, 3.5 g of NaCl, 14 g of Glucose, and 1 ml 100% Glycerol. Adjust pH to 7.4 and add water to a final volume of 200 ml and readjust pH if necessary. Before purification add 1 tablet of EDTA-free protease inhibitor (Roche

Diagnostics GmbH) and 50 μl 1 M DTT per 50 ml of buffer and incubate on ice.

3. Wash Buffer: 10 mM HNa_2PO_4, 300 mM NaCl, 30 mM imidazole, 1 mM DTT, pH 7.4. Prepare as previous step.
4. Labeling Buffer: 10 mM TCEP in PBS.
5. Cleavage buffer: 50 mM Tris-HCl, 150 mM NaCl, 1 mM EDTA, 1 mM DTT, pH 7.0.
6. Elution Buffer: 10 mM HNa_2PO_4, 300 mM NaCl, 300 mM imidazole, 1 mM DTT, pH 7.4. Prepare as in the previous step.
7. Ni-NTA Agarose beads.
8. 10 mM (tris(2-carboxyethyl)phosphine (TCEP)) in PBS.
9. AlexaFluor®-Maleimide in anhydrous dimethyl sulfoxide (DMSO). Dissolve AlexaFluor®-Maleimide in fresh DMSO to ~100 μM or as indicated by the company.
10. Glutathione-sepharose 4B beads in 20% ethanol (GE Healthcare Life Sciences).
11. PreScission protease in cleavage buffer + 20% glycerol (GE Healthcare Life Sciences).
12. LB Broth.
13. 1 M Isopropyl β-D-1-thiogalactopyranoside (IPTG) in water.
14. Shaking incubator.
15. Probe-type Sonicator for cell disruption equipped with a tip suited for 50 ml tubes.
16. Cooled Centrifuge (18,000 × *g*).

2.2 Fixation

Cultured cells grown on any surface that is compatible with TIRF imaging: e.g. epithelial cells or neurons plated on glass coverslips (*see* **Note 2**).

1. Cytoskeleton Buffer: 10 mM MES, 150 mM NaCl, 5 mM $MgCl_2$, 5 mM EGTA, 5 mM Glucose, pH 6.1 [15].
2. 16% w/v Paraformaldehyde (PFA) dissolved in water.
3. 1× d-PBS.
4. Fixation Buffer: Cytoskeleton buffer supplemented with 0.5% Triton-X and 3.7% w/v PFA.
5. Blocking solution: 3% w/v BSA in d-PBS.
6. Optional: antibodies for detection of additional structures.

2.3 Sample Preparation

1. Tweezers.
2. Mounting chamber.
3. d-PBS.
4. Purified lifeAct coupled to a fluorophore.

2.4 Microscope Setup

1. Standard inverted fluorescence microscopy equipped with a high NA objective and a total internal reflection fluorescence (TIRF) module.
2. Fluorescent filters for imaging GFP or the conjugated fluorophore.
3. Excitation lasers with the appropriate wavelength.
4. EMCCD camera or CMOS camera, sensitive enough to image single molecules.
5. SMLM software for super-resolution reconstruction: e.g. DoM Utrecht (Detection of Molecules, https://github.com/ekatrukha/DoM_Utrecht [19]), QuickPalm, (http://imagej.net/QuickPALM [20]), Thunderstorm (http://zitmen.github.io/thunderstorm/, [21]), RapidSTORM (http://www.super-resolution.biozentrum.uni-wuerzburg.de/research_topics/rapidstorm/, [22]), NIS Elements (Nikon instruments).
6. Microscope control via PC and dedicated software, for example Micromanager (https://micro-manager.org/, [23]).

3 Methods

3.1 Expression and Passivation on Ni-NTA Beads

The correct expression and purification protocols vary between the two different options, i.e. with or without GFP. Because lifeAct coupled to GFP is highly soluble, standard purification protocols and buffers are used. For the lifeAct without GFP, the full recombinant protein is bound to the Ni-NTA beads and the cysteine containing lifeAct fragment is cleaved off by PreScission protease after on-bead labeling. Subsequently free PreScission is captured by glutathione beads. Full recombinant protein coupled to GFP or the short lifeAct fragment coupled to an Alexa dye by the maleimide–-cysteine reaction can be obtained at high yields. However, it should be noted that the free cysteine, which was introduced in the construct, is prone to form disulfide bonds with other free cysteines in the samples, resulting in precipitation. To overcome this problem, reducing reagents like DTT or TCEP are required at all steps. A detailed step-by-step description of purification follows below.

1. Grow 0.8 l *E. coli* BL21DE3 containing the lifeAct expression plasmid to $OD_{0.6}$ at 37 °C from an overnight 4 ml culture in LB. Induce protein expression by addition of 800 µL 1 M IPTG to achieve a final concentration of 1 mM. Incubate for 3.5 h at 37 °C or 16 h overnight at 17 °C.
2. After induction, transfer the bacteria into a centrifuge compatible bucket and spin at 4000 × *g* for 30 min at 4 °C. Decant supernatant carefully and incubate pellet on ice. Resuspend

bacterial pellet in resuspension buffer supplemented with protease inhibitors (5 ml/gram bacterial pellet) and transfer to a 50 ml tube.

3. To lyse the bacteria, sonicate the bacterial suspension 5 × 1 min with 5 min intervals on ice. Intermediate to high sonication powers can be used.
4. Following sonication, the soluble fraction of the bacterial suspension can be separated from the insoluble sample fraction through centrifugation at 18,000 × *g* at 4 °C for 40 min (*see* **Note 3**).
5. During centrifugation wash 1.0 ml of Ni-NTA resin (0.5 ml Beads) in resuspension buffer. Beads can be centrifuged at 1000 × *g* for 3 min with slow deceleration. Supernatant can then be removed by a vacuum pump or pipet and replaced by resuspension buffer. Repeat the bead wash three times in resuspension buffer with 10× the bead resin volume (10 ml).
6. To separate the soluble fraction from the insoluble fraction after centrifugation, transfer the supernatant into a 50 ml tube to separate it from pellet. Typically, the supernatant of bacteria is a yellowish solution. However, because lifeAct is tagged with a GFP, the supernatant can appear more greenish. The pellet should be brown/yellowish, but can also be greenish because it can contain some aggregated protein or non-lysed expressing cells.
7. Add the washed Ni-NTA beads to the soluble supernatant and incubate at 4 °C while gently rolling for 2 h. The His-Tag of the recombinant lifeAct will bind to the beads.
8. After incubation spin the beads at 1000 × *g* for 3 min with slow deceleration as described before. The lifeAct-Cys-PreScission-Site-GFP-6×His is now bound to the beads. Supernatant containing all other soluble proteins that do not contain a His-Tag can be discarded.
9. Wash the beads three times as described above in wash buffer to reduce nonspecific interactions of proteins with the beads. The lifeAct recombinant fragment has 6×His-Tag which binds tightly to Ni-NTA. This specific interaction will not be disrupted by the 30 mM imidazole in the wash buffer.

3.2 Purification with GFP

1. To obtain the full lifeAct-Cys-PreScissionSite-GFP-6×His for SMLM (*see* **Note 4**), the recombinant protein can be eluted by aspiration of the last wash step as described in Subheading 3.1. Addition of 3.5 ml Elution Buffer results in the elution of the recombinant His-tagged protein from the beads after 10 min incubation. Beads can be spun down and the supernatant containing lifeAct-GFP can be collected.

2. The eluted fraction can be used directly for SMLM as described in Subheading 3.5. For long-term storage, exchange the buffer to PBS + 1 mM DTT using a buffer exchange column, and add 10% glycerol. Snap-freezing followed by −80 °C storage is recommended. The purity of the final sample can be determined by SDS-page. Typically, this approach yields highly pure samples.

3.3 Labeling and Purification with Organic Dyes

The second mode in which this recombinant lifeAct fragment can be used is by labeling of the introduced cysteine through a maleimide–thiol interaction. The lifeAct-Cys, coupled to the thiol, can subsequently be cleaved off the GFP-6×His and further purified. The overall advantage is that almost all organic dyes and other chemical modifications are available conjugated to a maleimide. Therefore it can be used to label the lifeAct-Cys fragment with a variety of stable fluorophores, resulting in a high photon yield. Below we describe how the cysteine can be labeled with an Alexa647 through maleimide coupling on the beads, followed by cleavage at the PreScission site.

1. After the third wash in wash buffer (Subheading 3.1) wash the beads three additional times with labeling buffer. Because DTT contains two thiol groups, it is not compatible with maleimide coupling. Replacement with of DTT with TCEP is therefore essential for protein solubility and coupling efficiency.
2. For labeling, aspirate the final wash and transfer the beads into a 2 ml Eppendorf. Add 1000 μl labeling buffer supplemented with 80 μl of ~100 μM Alexa647-maleimide (~8 nmol Alexa647) in DMSO and incubate for 4 h at room temperature. After incubation add an additional 60 μL ~100 μM Alexa647-maleimide and incubate overnight at 4 °C. The maleimide-dye is added in excess and should, if incubation times are long enough, label almost all free cysteines in the sample.
3. Remove excess dye after labeling through three 1 ml washes in Cleavage Buffer. This buffer allows optimal cleavage at the PreScission cleavage site, releasing lifeAct-Cysteine labeled with Alexa647 while leaving GFP-6×His bound to the beads.
4. Cleave lifeAct-Cys-Alexa647 from the Ni-NTA beads by replacing the final wash step with 70 μL PreScission protease in 500 μL Cleavage Buffer for 5 h at 4 °C (or overnight) while gently rolling.
5. While cleaving, wash 250 μl glutathione beads with cleavage buffer as described above.
6. Capture PreScission protease on the glutathione beads by addition of the prewashed beads to the sample. Now, both PreScission and the GFP-6×His are bound to the glutathione and Ni-

NTA beads respectively while lifeAct-Cys-Alexa647 diffuses in the supernatant.

7. The supernatant containing soluble lifeAct-Cys-A647 can be collected. The final concentration of the lifeAct peptide can be determined using the Bicinchoninic Acid (BCA) protein assay [24]. The labeling efficiency can then be determined by measuring the dye concentration by spectroscopy and application of Beer-Lambert's law. Typical concentrations of labeled lifeAct range from 0.1 to 1 μM (*see* **Note 5**).
8. Finally, supplement the sample with a final concentration of 10% glycerol, snap-freeze in liquid nitrogen and store at −80 °C.

3.4 Sample Preparation

Because in super resolution all details and therefore also sample errors are visualized, optimized sample preparation and dense label coverage are essential for a successful final reconstruction. Fixations and staining protocols that would result in a smooth diffraction limited image might result in sparsely labeled structures in super resolution. Sample preparation should therefore be optimized for each individual structure or co-labeling of multiple structures. The buffer conditions during fixation also play an important role to preserve cytoskeletal structures. Whereas microtubule fixations are preferentially performed in PEM80 buffer [25], cytoskeleton buffer is the fixation buffer of choice for actin [15, 17]. Finally, fixatives should be chosen carefully and such that labeling is not perturbed and structures are maintained. Actin structures are preferentially fixed by PFA or Glutaraldehyde [26]. Below a simple and fast sample preparation is described with PFA in cytoskeletal buffer to preserve the actin network.

1. Pre-warm fixation buffer to 37 °C. Remove the medium from the cells coated on coverslips and gently add pre-warmed fixation buffer for 10 min. Triton-X ensures sufficient permeabilization of the cells, resulting in release of cytoplasm which allows the lifeAct probe to diffuse freely. Simultaneously, PFA fixes cellular structures like actin.
2. After fixation aspirate the fixation buffer and wash the sample with d-PBS for 5 min. Even though the samples are fixed, pipet with care not to perturb the samples. Repeat the wash three times.
3. After washing, block the sample with blocking solution for at least 30 min at room temperature. Blocking reduces the number of unspecific protein–protein interactions reducing the background signal in the final image.
4. To stain for structures additional to actin, the samples can be further incubated with antibodies after blocking. Antibodies compatible with PFA fixation can be diluted in blocking

solution and incubated on the sample for at least 1 h at room temperature. Subsequently, the primary antibody incubation can be stopped by three additional 5-min washes with d-PBS. Cells can then be incubated with a suitable secondary labeled antibody in blocking solution to finish the staining for the desired structure (*see* **Note 6**).

5. After blocking and optional staining, the samples are ready to be mounted in d-PBS + DTT (*see* **Note 7**). A suitable chamber that is compatible with the microscope stage can be used. Open chambers like Ludin chambers for 18 mm round coverslips provide easy access to the imaging medium and allows for the addition or dilution of the lifeAct probe during image acquisition.

3.5 Imaging

1. Secure a sample on the microscope and select a position of interest. Before image acquisition can be started, it is important to select the correct parameters for an optimal super-resolution image. Focusing before acquisition is important to image the correct plane of interest. Because the low concentration of lifeAct used for imaging does not provide a full overview of the cellular outline a co-transfection or staining of an additional marker is favorable. Alternatively, an excess of lifeAct conjugated to a fluorophore can be added to the sample which results in a faint outline of the cellular actin structures. If the latter is applied, the concentration should be strongly reduced through dilution and bleaching before SMLM acquisition to be able to visualize single molecules (*see* **Note 8**).
2. For an optimal super-resolution acquisition carefully take the following parameters into account. Optimizing each condition carefully every time can increase the signal-to-noise ratio per imaging session:
   (a) *Exposure time*. For super resolution based on probe exchange, the on- and off-rates should guide the exposure time. Low off rates allow for high exposure times and collection of more photons. However, a single molecule binding event should not be obscured by another molecule binding in the vicinity rendering the software unable to detect them both as separate localizations. The latter has a higher chance at higher on rates. Therefore, a balanced exposure time is necessary. For lifeAct the reported half-life on the actin filaments is 23 ms [17] and it is preferentially imaged with 50–100 ms exposure time.
   (b) *Laser Power*. Laser power and exposure time are co-dependent on each other and on fluorophore stability. Fluorescent proteins like GFP are easily bleached compared to organic dyes. It is important that a maximum

amount of photons is collected from one single molecule during the selected exposure time. Therefore, laser power can be varied between probes with higher laser powers for more stable probes (*see* **Note 7**). Because the sample is crowded with diffusing lifeAct-fluorophore molecules the laser power should also be kept at moderate levels to minimize background. Starting at low laser powers and gradually increasing them usually results in the rapid recognition of the optimum laser power.

(c) *Number of collected frames*. The more frames can be collected, the better. Reconstruction of a single-molecule image preferentially relies only on the most accurate localizations, which can be filtered based on localization precision. Collecting more frames at optimal settings allows more stringent filters on localization precision, but care should be taken to minimize and correct sample drift. Selecting only the most accurate detection already results in a full overview of the image with high resolution. Typically we record 30,000–40,000 frames.

(d) *Fluorophore density*. SMLM relies on the detection of individual fluorophores conjugated to lifeAct that are binding sequentially. Therefore, lifeAct should be diluted to a concentration such that in every frame single molecules can be observed. In 2D and 3D imaging the plane in focus will be the plane where the point spread function of the single molecules is symmetrical. For SMLM imaging, labeled lifeAct is typically diluted to 1–5 nM in d-PBS (*see* **Note 9**).

(e) *Laser angle*. Total Internal Reflection of the laser at the coverslip–sample interface results in an evanescent wave of typically a few hundred nanometers, which prevents excitation of out-of-focus fluorophores. Reducing the incident laser angle results in a more oblique illumination field which yields deeper sample penetration and fluorophore excitation. The latter can be favorable because of imaging depth, but also increases background fluorescence. The incident laser angle should thus be adjusted dependent on required imaging depth and the background intensity that is acceptable.

3.6 Analysis

The final super-resolution image is created by accumulation of all single-molecule positions that were acquired during imaging. Single-molecule positions can be accurately determined by fitting the PSF to a Gaussian and determine the midpoint. The midpoint can be localized with nanometer precision based on the width of the Gaussian. Detection/fitting and subsequent reconstruction of the super-resolved image is performed by dedicated software

packages. There are several freely available packages (e.g. DoM Utrecht [19], RapidSTORM [22], ThunderSTORM [21], QuickPALM [20]) or commercially available packages to reconstruct a super-resolved image.

1. Detection and fitting of the imaged fluorophores is dependent on the image parameters as well as on the recorded PSF. The software usually requires input of the pixel size and several threshold values like estimated PSF size to exclude abnormal detections that cannot result from single molecules. The midpoint of included localizations is then determined with nanometer precision by fitting or maximum likelihood estimation.
2. The detection and fitting process results in a table that contains information about all the individual detected fluorophores. Fluorophore parameters include: the *x*- and *y*-coordinate, the image number in which it was acquired, PSF symmetry (in *x* and *y*), PSF shape, PSF brightness etc.
3. Next, reconstruction of the super-resolution image can be done based on this particle table. All the stored *x*- and *y*-coordinate are used to plot the midpoint of these molecules. The midpoint can be plotted as a small Gaussian of a constant size or each midpoint can be plotted as a spot based on its individual localization error. This localization error can be calculated from the fitting parameters and used as a threshold. Fluorophores with more precise localizations can then be plotted as tight spots while less well localized fluorophores are represented as more spread localizations. Several parameters should be taken into account while reconstructing the final image. The pixel size of the reconstructed image should be selected in such a way that they are at least half the size of the smallest details according to the Nyquist criterion. Furthermore, the localizations used in the final reconstruction can be filtered on the localization precision. It should be noted that filtering too much or selecting a very low pixel size will eventually result in very sparse localizations. Both these parameters can be varied and optimized per image to obtain a successful and informative super-resolution reconstruction.
4. Drift correction is a final important step in the analysis. Because of the nanometer localization accuracy, any drift of the sample with respect to the objective will be clearly visible in the final reconstruction. Long imaging times combined with small thermal fluctuations will result in noticeable drift in the final reconstruction. The available software packages usually support drift correction based on frame-to-frame cross-correlation of fiducial markers or cross-correlation of intermediate super-resolution reconstructions [27, 28]. The fiducial markers can be small particles like beads that are fixed to the coverslip and do not

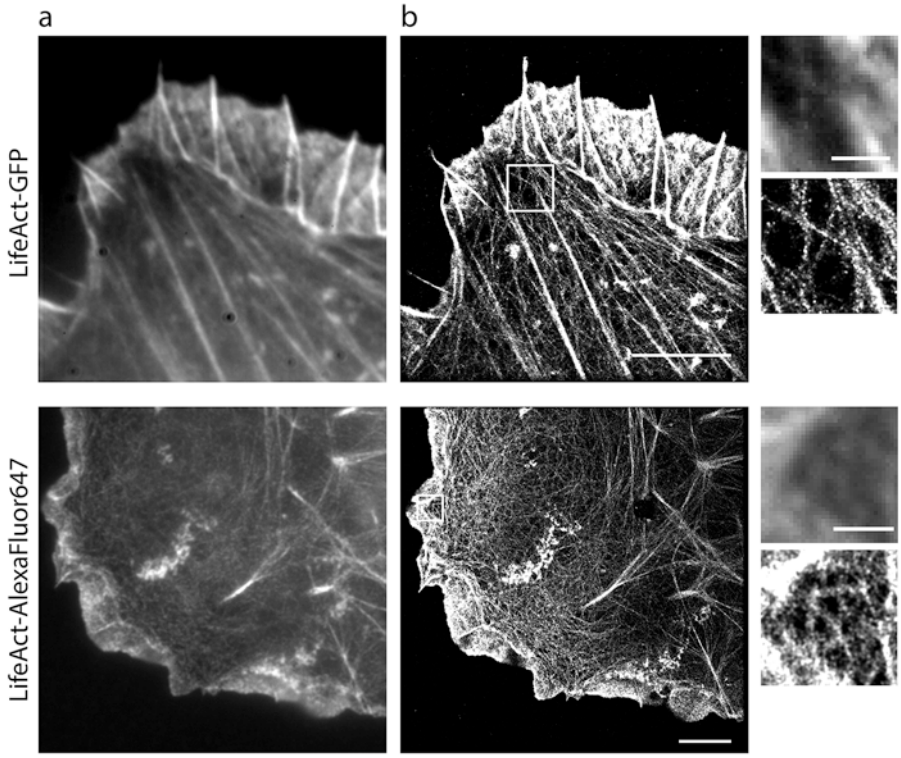

Fig. 2 Representative super-resolution images obtained using the lifeAct probes. Diffraction-limited overview **(a)**, super-resolved image **(b)**, and zooms of lifeAct-GFP used on a HeLa cell (*top*) or lifeAct-AlexaFluor647 used on a COS7 cell (*bottom*). Scale bars in super-resolved images are 5 μm in **a** and **b** and 1 μm in the zooms

move within the sample. When drift correction based on intermediate super-resolution reconstructions is applied, a frame interval should be chosen in such a way that the images can be correctly correlated and drift can be detected (*see* **Note 9**).

5. An example of a successful super-resolution reconstruction of actin, imaged with either GFP or Alexa647 coupled to lifeAct is shown in Fig. 2.

4 Notes

1. The amino acid sequence of the **lifeAct**-cysteine-***PreScission-Site***-GFP-6×His construct is
MGVADLIKKFESISKEEGSGS**C**EF***LEVLFQGP***VSKGEEL
FTGVVPILVELDGDVNGHKFSVSGEGEGDATYGKLTLK
FICTTGKLPVPWPTLVTTLTYGVQCFSRYPDHMKQHDF
FKSAMPEGYVQERTIFFKDDGNYKTRAEVKFEGDTLVRI
ELKGIDFKEDGNILGHKLEYNYNSHNVYIMADKQKNGI

KVNFKIRHNIEDGSVQLADHYQQNTPIGDGPVLLPDNH
YLSTQSKLSKDPNEKRDHMVLLEFVTAAGITLGMDELYK
LEHHHHHH

2. Identifying cells of interest. Because low concentrations of lifeAct do not provide a full overview of the cellular structures, a fill or other cellular marker can be expressed to identify cells of interest.
3. Optimizing protein yields.
   (a) A greenish bacterial pellet usually indicates sufficient expression.
   (b) During each step samples for SDS page can be taken to determine the presence of recombinant protein.
   (c) Release of soluble protein after lysis can be increased by the addition of small amounts of lysozyme to weaken the bacterial cell wall.
   (d) Overall low soluble protein levels can occur because the recombinant lifeAct can enter into inclusions bodies at too high concentrations. This can be prevented by reducing induction time to only a few hours at 20 °C. In addition, DTT concentration can be increased to prevent disulfide-bond formation after lysis.
4. Alternative construct for fluorescent protein imaging only. When lifeAct is only used conjugated to GFP or other fluorescent proteins, removal of the cysteine and PreScission site could result in higher solubility and protein yields.
5. In case of low labeling efficiency of lifeAct-Cysteine:
   (a) Measure the amount of labeled lifeAct by BCA assay and the concentration of labeled lifeAct as described in Subheading 3.4. When the protein concentration is much higher than the concentration of the fluorophore, the sample is most likely unsaturated due to an inefficient maleimide–thiol reaction or because too little dye was added during the reaction. In the latter case, repeat the purification with an increased dye concentration. The fluorophore to lifeAct-cysteine ratio should be 10–20.
   (b) In case of poor reaction efficiency, also check the pH of the buffers. Furthermore, make sure that DTT is washed from the solution and that TCEP exceeds the protein concentration approximately tenfold to reduce unwanted disulfide bond formation of the available cysteines.
6. Alternative protocol for multicolor super resolution:
   (a) Alternative to the protocol described in Subheading 3.4 an extraction and fixation protocol more optimal for co-staining with microtubules can be used. In Short: pre-

extract in 0.25% glutaraldehyde + 0.3% Triton-X in PEM80 for 1 min (37 °C). Replace pre-extraction with 4% PFA in PEM80 (37 °C) for 7 min. Proceed with washing as described in Subheading 3.4 and add an extra permeabilization step of 0.25% Triton-X in d-PBS for 8 min followed by three more washes and blocking. Use primary labeled antibodies or nanobodies against tubulin to speed up the staining process [19].

(b) Secondary antibodies can be labeled with a variety of functionalized probes. When super-resolution imaging of actin by lifeAct needs to be combined with dSTORM super-resolution imaging of the second structure, Alexa647 is the best label to be used on the secondary antibody. Alexa647 has rapid blinking properties in PBS supplemented with glucose oxygen scavenger [25]. LifeAct-based protein-PAINT is compatible with this buffer.

7. The rapid blinking properties make Alexa647 extremely suitable for dSTORM. However, when lifeAct-Cysteine is used for PAINT-like super resolution through transient binding a more stable fluorophore is required. Labeling lifeAct-Cysteine with other organic dyes might result in a higher photon yield. Alternatively, addition of methylviologen (MV) and ascorbic acid (AA) in the imaging buffer will stabilize Alexa647 significantly [29, 30]. Concentrations of MV and AA can be varied between 50 μM and 1 mM to optimize photon yield and binding properties.
8. Cell morphology and structures appear to be affected after fixation. Handle samples carefully. Samples are very fragile during extraction and fixation. Always pipet at the sides of the dish and not directly on the sample because sheer stress can perturb the cell integrity even when fixed. Take extra care while handling samples that are sensitive to fixation techniques like neurons and thick samples.
9. Super-resolution reconstruction is unclear:
   (a) SMLM relies on the localizations of truly individual fluorophores. Too little localizations will result in a dotty image that can be enhanced by an increase of the pixel size. This will increase the amount of localizations per pixels. However, labeling density can also be too high. When two fluorophores emit light too close together the PSFs will obscure each other and result in mislocalization and poor localization errors. False and poorly localized detections will result in a loss of details.
   (b) Adjust drift interval and other parameters of drift correction. Incorrect drift correction can be clearly visible as a jumped image but sometimes also more subtle as a blurry reconstruction.

References

1. Arnold DB, Gallo G (2014) Structure meets function: actin filaments and myosin motors in the axon. J Neurochem 129(2):213–220. doi:10.1111/jnc.12503
2. Kapitein LC, Schlager MA, Kuijpers M, Wulf PS, van Spronsen M, MacKintosh FC, Hoogenraad CC (2010) Mixed microtubules steer dynein-driven cargo transport into dendrites. Curr Biol 20(4):290–299. doi:10.1016/j.cub.2009.12.052
3. Vale RD (2003) The molecular motor toolbox for intracellular transport. Cell 112(4):467–480
4. Crawley SW, Mooseker MS, Tyska MJ (2014) Shaping the intestinal brush border. J Cell Biol 207(4):441–451. doi:10.1083/jcb.201407015
5. Kapitein LC, Hoogenraad CC (2015) Building the neuronal microtubule cytoskeleton. Neuron 87(3):492–506. doi:10.1016/j.neuron.2015.05.046
6. Kapitein LC, van Bergeijk P, Lipka J, Keijzer N, Wulf PS, Katrukha EA, Akhmanova A, Hoogenraad CC (2013) Myosin-V opposes microtubule-based cargo transport and drives directional motility on cortical actin. Curr Biol 23(9):828–834. doi:10.1016/j.cub.2013.03.068
7. Watanabe K, Al-Bassam S, Miyazaki Y, Wandless TJ, Webster P, Arnold DB (2012) Networks of polarized actin filaments in the axon initial segment provide a mechanism for sorting axonal and dendritic proteins. Cell Rep 2(6):1546–1553. doi:10.1016/j.celrep.2012.11.015
8. Hell SW (2007) Far-field optical nanoscopy. Science 316(5828):1153–1158. doi:10.1126/science.1137395
9. Huang B, Babcock H, Zhuang X (2010) Breaking the diffraction barrier: super-resolution imaging of cells. Cell 143(7):1047–1058. doi:10.1016/j.cell.2010.12.002
10. Rust MJ, Bates M, Zhuang X (2006) Sub-diffraction-limit imaging by stochastic optical reconstruction microscopy (STORM). Nat Methods 3(10):793–795. doi:10.1038/nmeth929
11. Betzig E, Patterson GH, Sougrat R, Lindwasser OW, Olenych S, Bonifacino JS, Davidson MW, Lippincott-Schwartz J, Hess HF (2006) Imaging intracellular fluorescent proteins at nanometer resolution. Science 313(5793):1642–1645. doi:10.1126/science.1127344
12. Heilemann M, van de Linde S, Schuttpelz M, Kasper R, Seefeldt B, Mukherjee A, Tinnefeld P, Sauer M (2008) Subdiffraction-resolution fluorescence imaging with conventional fluorescent probes. Angew Chem 47(33):6172–6176. doi:10.1002/anie.200802376
13. Folling J, Bossi M, Bock H, Medda R, Wurm CA, Hein B, Jakobs S, Eggeling C, Hell SW (2008) Fluorescence nanoscopy by ground-state depletion and single-molecule return. Nat Methods 5(11):943–945. doi:10.1038/nmeth.1257
14. Jungmann R, Avendano MS, Woehrstein JB, Dai M, Shih WM, Yin P (2014) Multiplexed 3D cellular super-resolution imaging with DNA-PAINT and Exchange-PAINT. Nat Methods 11(3):313–318. doi:10.1038/nmeth.2835
15. Xu K, Zhong G, Zhuang X (2013) Actin, spectrin, and associated proteins form a periodic cytoskeletal structure in axons. Science 339(6118):452–456. doi:10.1126/science.1232251
16. Molle J, Raab M, Holzmeister S, Schmitt-Monreal D, Grohmann D, He Z, Tinnefeld P (2016) Superresolution microscopy with transient binding. Curr Opin Biotechnol 39:8–16. doi:10.1016/j.copbio.2015.12.009
17. Kiuchi T, Higuchi M, Takamura A, Maruoka M, Watanabe N (2015) Multitarget super-resolution microscopy with high-density labeling by exchangeable probes. Nat Methods 12(8):743–746. doi:10.1038/nmeth.3466
18. Riedl J, Crevenna AH, Kessenbrock K, JH Y, Neukirchen D, Bista M, Bradke F, Jenne D, Holak TA, Werb Z, Sixt M, Wedlich-Soldner R (2008) Lifeact: a versatile marker to visualize F-actin. Nat Methods 5(7):605–607. doi:10.1038/nmeth.1220
19. Mikhaylova M, Cloin BM, Finan K, van den Berg R, Teeuw J, Kijanka MM, Sokolowski M, Katrukha EA, Maidorn M, Opazo F, Moutel S, Vantard M, Perez F, van Bergen en Henegouwen PM, Hoogenraad CC, Ewers H, Kapitein LC (2015) Resolving bundled microtubules using anti-tubulin nanobodies. Nat Commun 6:7933. doi:10.1038/ncomms8933
20. Henriques R, Lelek M, Fornasiero EF, Valtorta F, Zimmer C, Mhlanga MM (2010) QuickPALM: 3D real-time photoactivation nanoscopy image processing in ImageJ. Nat Methods 7(5):339–340. doi:10.1038/nmeth0510-339
21. Ovesny M, Krizek P, Borkovec J, Svindrych Z, Hagen GM (2014) ThunderSTORM: a comprehensive ImageJ plug-in for PALM and STORM data analysis and super-resolution

imaging. Bioinformatics 30(16):2389–2390. doi:10.1093/bioinformatics/btu202

22. Wolter S, Loschberger A, Holm T, Aufmkolk S, Dabauvalle MC, van de Linde S, Sauer M (2012) rapidSTORM: accurate, fast open-source software for localization microscopy. Nat Methods 9(11):1040–1041. doi:10.1038/nmeth.2224
23. Edelstein A, Amodaj N, Hoover K, Vale R, Stuurman N (2010) Computer control of microscopes using microManager. Curr Protoc Mol Biol Chapter 14:Unit14 20. doi:10.1002/0471142727.mb1420s92
24. Olson BJ, Markwell J (2007) Assays for determination of protein concentration. Curr Protoc Protein Sci Chapter 3:Unit 3 4. doi:10.1002/0471140864.ps0304s48
25. Yau KW, van Beuningen SF, Cunha-Ferreira I, Cloin BM, van Battum EY, Will L, Schatzle P, Tas RP, van Krugten J, Katrukha EA, Jiang K, Wulf PS, Mikhaylova M, Harterink M, Pasterkamp RJ, Akhmanova A, Kapitein LC, Hoogenraad CC (2014) Microtubule minus-end binding protein CAMSAP2 controls axon specification and dendrite development. Neuron 82(5):1058–1073. doi:10.1016/j.neuron.2014.04.019
26. Leyton-Puig D, Kedziora KM, Isogai T, van den Broek B, Jalink K, Innocenti M (2016) PFA fixation enables artifact-free super-resolution imaging of the actin cytoskeleton and associated proteins. Biol Open 5(7):1001–1009. doi:10.1242/bio.019570
27. Lee SH, Baday M, Tjioe M, Simonson PD, Zhang R, Cai E, Selvin PR (2012) Using fixed fiduciary markers for stage drift correction. Opt Express 20(11):12177–12183. doi:10.1364/OE.20.012177
28. Mlodzianoski MJ, Schreiner JM, Callahan SP, Smolkova K, Dlaskova A, Santorova J, Jezek P, Bewersdorf J (2011) Sample drift correction in 3D fluorescence photoactivation localization microscopy. Opt Express 19(16):15009–15019. doi:10.1364/OE.19.015009
29. Vaughan JC, Jia S, Zhuang X (2012) Ultrabright photoactivatable fluorophores created by reductive caging. Nat Methods 9(12):1181–1184. doi:10.1038/nmeth.2214
30. Vogelsang J, Kasper R, Steinhauer C, Person B, Heilemann M, Sauer M, Tinnefeld P (2008) A reducing and oxidizing system minimizes photobleaching and blinking of fluorescent dyes. Angew Chem 47(29):5465–5469. doi:10.1002/anie.200801518